 MCB, vol.2, no.4, pp.191-204, 2005

The Effect of Matrix Tension-Compression Nonlinearity and Fixed Negative Charges on Chondrocyte Responses in Cartilage

Morakot Likhitpanichkul [1], X. Edward Guo [2], and Van C. Mow[1, 3]

Abstract: Thorough analyses of the mechano-electrochemical interaction between articular cartilage matrix and the chondrocytes are crucial to understanding of the signal transduction mechanisms that modulate the cell metabolic activities and biosynthesis. Attempts have been made to model the chondrocytes embedded in the collagen-proteoglycan extracellular matrix to determine the distribution of local stress-strain field, fluid pressure and the time-dependent deformation of the cell. To date, these models still have not taken into account a remarkable characteristic of the cartilage extracellular matrix given rise from organization of the collagen fiber architecture, now known as the tension-compression nonlinearity (TCN) of the tissue, as well as the effect of negative charges attached to the proteoglycan molecules, and the cell cytoskeleton that interacts with mobile ions in the interstitial fluid to create osmotic and electro-kinetic events in and around the cells. In this study, we proposed a triphasic, multi-scale, finite element model incorporating the Conewise Linear Elasticity that can describe the various known coupled mechanical, electrical and chemical events, while at the same time representing the TCN of the extracellular matrix. The model was employed to perform a detailed analysis of the chondrocytes' deformational and volume responses, and to quantitatively describe the mechano-electrochemical environment of these cells. Such a model describes contributions of the known detailed micro-structural and composition of articular cartilage. Expectedly, results from model simulations showed substantial effects of the matrix TCN on the cell deformational and volume change response. A low compressive Poisson's ratio of the cartilage matrix exhibiting TCN resulted in dramatic recoiling behavior of the tissue under unconfined compression and induced significant volume change in the cell. The fixed charge density of the chondrocyte and the pericellular matrix were also found to play an important role in both the time-dependent and equilibrium deformation of the cell. The pericellular matrix tended to create a uniform osmolarity around the cell and overall amplified the cell volume change. It is concluded that the proposed model can be a useful tool that allows detailed analysis of the mechano-electrochemical interactions between the chondrocytes and its surrounding extracellular matrix, which leads to more quantitative insights in the cell mechano-transduction.

keyword: Articular cartilage, Cell-Matrix interaction, Triphasic theory, Tension-Compression nonlinearity, Multi-scale finite element model, Fixed charge density, Unconfined compression.

1 Introduction

Articular cartilage is an efficiently designed load-bearing material, consisting of mostly water that resides within the interstices of an entangled network of collagen fibers (primarily type II) and negatively charged proteoglycans. The cartilage extracellular matrix (ECM) shows a depth-dependent ultrastructure due to specific orientations of its collagen fibers, which is parallel to the articular surface in the superficial zone, random in the middle zone, and perpendicular to the calcified interface in the deep zone [Mow, Gu and Chen (2005)]. The complex composition and micro-architecture of the cartilage ECM provides the tissue its special biomechanical properties necessary to withstand high joint loading throughout the tissue's lifespan. Embedded within the cartilage extracellular matrix is a sparse population of chondrocytes, which have the ability to remodel the matrix in response to

[1] The Liu Ping Laboratory for Functional Tissue Engineering Research, Department of Biomedical Engineering, Columbia University, New York, NY

[2] Bone Bioengineering Laboratory, Department of Biomedical Engineering, Columbia University, New York, NY

[3] Corresponding author, Stanley Dicker Professor and Chair, Department of Biomedical Engineering, Columbia University, 351 Engineering Terrace 500 West 120^{th} Street, New York, NY 10027. Telephone: (212) 854-8462 Fax: (212) 854-8725 Email: vcm1@columbia.edu

changes in joint loading history [Guilak, Sah and Setton (1997)]. Under physiologic joint loading, complex mechanical, electrical and chemical events (e.g., stress, strain, fluid and osmotic pressures, ion flows, electrical current and electrical potential) are generated throughout the cartilage tissue. Under pathological conditions such as osteoarthritis, these mechano-electrochemical (MEC) events are altered significantly due to changes in tissue composition following break-down of collagen fibers, excessive hydration, loss or changes in molecular conformations of proteoglycans. The chondrocytes experience these environmental changes through complicated mechanisms of cell-matrix interaction (e.g. direct stress transmission from ECM through intracellular structure to its nucleus, membrane-bound receptors, stretch and pressure activated ion channels, biochemical messengers, etc) and perceive them as signals to alter the metabolic and biosynthesis activities, which in turn affect the development and progression of the disease itself, [Sandy, Adams, Billingham et al. (1984); Ratcliffe, Beauvais and Saed-Nejad (1994)]. It is crucial to know and thoroughly understand the mechano-electrochemical (MEC) interactions between the cartilage extracellular matrix and the chondrocytes in order to develop meaningful insights in the mechanisms of the signal transduction underlying the biological adaptation and degeneration of cartilage, which has remain unclear to date.

In attempt to study the chondrocyte responses to physicochemical stimulations, numerous studies have investigated changes in the cell biosynthesis in cartilage explants and chondrocyte-hydrogel constructs following specific loading configurations such as hydrostatic pressure, mechanical compression, shear and osmotic stress e.g., [Lammi, Inkinen, Parkkinen et al. (1994); Bachrach, Valhmu, Stazzone et al. (1995); Buschmann, Gluzband, Grodzinsky et al. (1995); Guilak, Sah and Setton (1997); Wong, Wuethrich, Buschmann et al. (1997); Quinn, Grodzinsky, Buschmann et al. (1998); Mauck, Soltz, Wang et al. (2000); Wu and Chen (2000); Jin, Frank, Quinn et al. (2001); Palmer, Chao Ph, Raia et al. (2001); Hung, LeRoux, Palmer et al. (2003); Waldman, Spiteri, Grynpas et al. (2003); Szafranski, Grodzinsky, Burger et al. (2004)]. However, even though the loading configuration in a tissue explant experiment seems to be simple and clearly defined, in almost all cases the resulting *in situ* MEC fields around the cell are still highly complex and difficult to analyze. In order to quantify the local environment around the cell within the tissue resulting from the applied load to the cartilage surface, accurate constitutive models for both the cartilage matrix and the cell, together with elaborate computational tools are required to simulate the MEC interactions between the cell and the ECM. Previously, a number of models on the cell-matrix mechanical interaction have been created. For instance, Bachrach and coworkers [Bachrach, Valhmu, Stazzone et al. (1995)] modeled the chondrocytes, using the biphasic theory [Mow, Kuei, Lai et al. (1980)], as fluid-solid inclusions embedded in and attached to a biphasic ECM of distinct material properties, while the tissue is subjected to a confined compression test. They obtained a closed-form analytical solution following the solution of spherical elastic inclusions by Goodier .[Goodier (1937)]. Subsequently, Guilak and Mow [Guilak and Mow (2000)] employed a biphasic finite element model, together with a multi-scale numerical algorithm to analyze the mechanical environment of the chondrocyte in cartilage under unconfined compression. This kind of multi-scale model allows calculations of such a complex problem involving a large range of the geometric scales from the tissue level to the cell level (2 orders of magnitude difference). Results from their thorough parametric studies on the material properties of the chondrocyte, the pericellular matrix (PCM) and the ECM demonstrated a significant effect of these parameters on the cell mechanical environment, and suggested a functional biomechanical role of the PCM. Similarly, Wu and Herzog [Wu and Herzog (2000)] also utilized a multiscale biphasic finite element model method, extended into 3D, to determine the cell deformational response at the center and the edge of a cartilage-bone plug under unconfined compression. They also accounted for the influence of cell volumetric fraction on cartilage mechanical properties, as well as performed the analysis using finite deformation approach. These models however are all based on the biphasic theory that did not account for the effect of negative charges and mobile ions that give rise to the physicochemical and electrical events surrounding the cells, which are also known to be important factors modulating the cell activities [Chao, Roy, Mauck et al. (2000); Palmer, Chao Ph, Raia et al. (2001); Hung, LeRoux, Palmer et al. (2003)]. A major advance in constitutive modeling of charged-hydrated, porous-permeable materials is the development of a multiphasic mixture theory used to describe tissues such as cartilage; this is known as the triphasic theory [Lai, Hou and Mow (1991)]

(a)

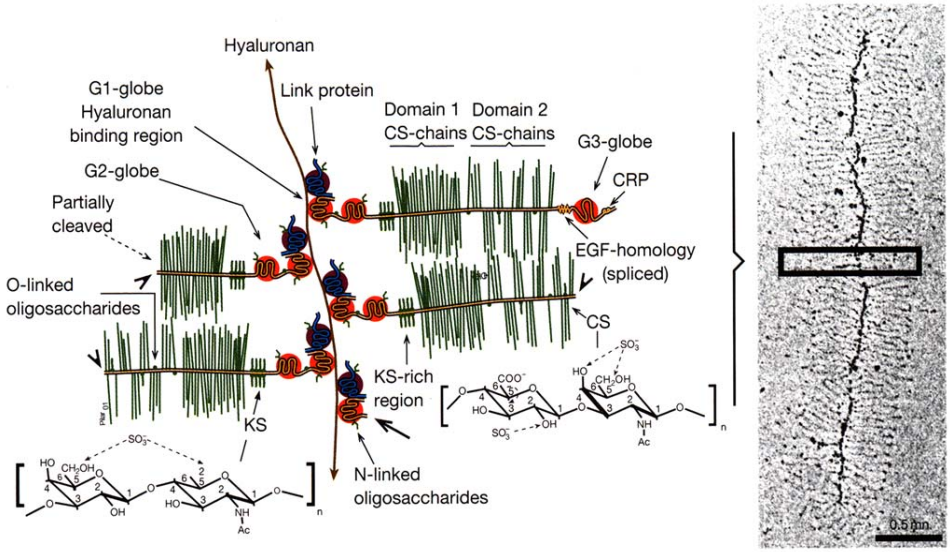

(b)

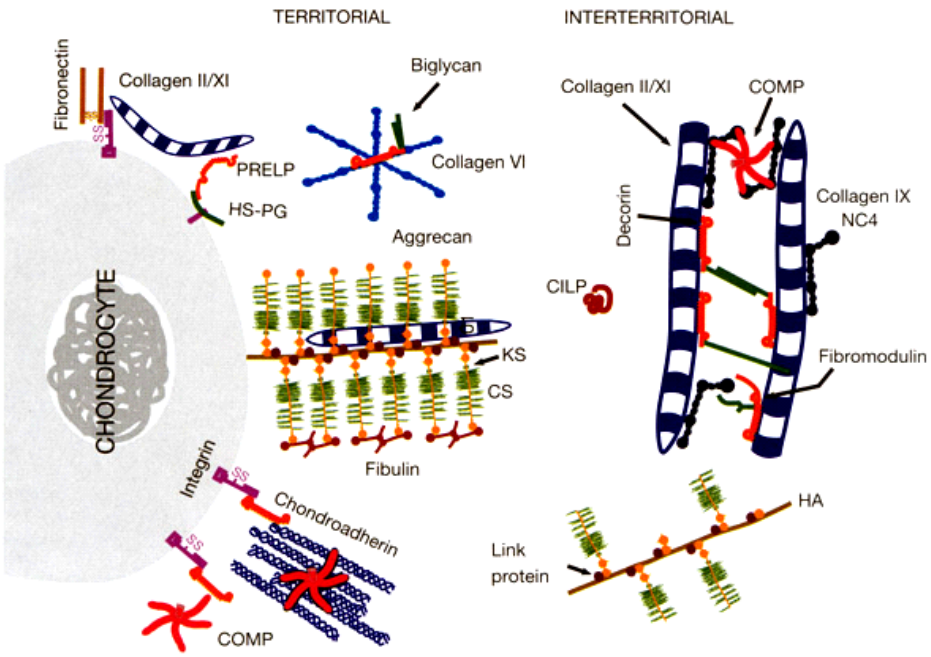

Figure 1 : (a) Proteoglycan macromolecule, (b) The macromolecules of a cartilaginous extracellular matrix, their relationships with each other, and with chondrocytes. The structural load supporting macromolecules of articular cartilage are collagen of various types (II, V, VI, IX, XI) and the proteoglycans . Type II collagen phenotypically defines articular cartilage. Charges derived from carboxyl (COO^-) and sulfate (SO_4^{2-}) groups are fixed to the glycosaminoglycans attached to the protein cores of the proteoglycan. Other glycosaminoglycans include COMP, hyaluronan, fibromodulin, decorin, and biglycan. [Heinegard, Bayliss and Lorenzo (2003)]

and it allowed analysis of the complex MEC field within cartilage. In more recent times, advances in constitutive modeling based on the triphasic theory have focused on tissue inhomogeneities and anisotropies e.g., [Huang,

Soltz, Kopacz et al. (2003); Wang, Chahine, Hung et al. (2003)] and on tissue permeability e.g., [Gu and Yao (2003); Gu, Yao, Huang et al. (2003)]. The theoretical framework used for these latter advances is the triphasic constitutive theory, though with emphasis on experimental data defining tissue inhomogeneities and anisotropies, and subsequent improvements in the fidelity of predictions with experimental data. These recent advances thus have been incorporated to reveal their influences on the mechanical, electrical and chemical signals that the chondrocytes might see within cartilage under various mechanical loadings [Mow, Wang and Hung (1999); Wang, Guo, Sun et al. (2002)]. Results from the recent analyses further confirmed that fixed negative charges and mobile ions played an important role in the MEC field within the tissue and should not be neglected. Recently, Lai and coworkers were able to employ a multi-scale finite element model based on the triphasic theory to quantify electrical signals for chondrocytes within cartilage under confined compression [Lai, Sun, Ateshian et al. (2002)].

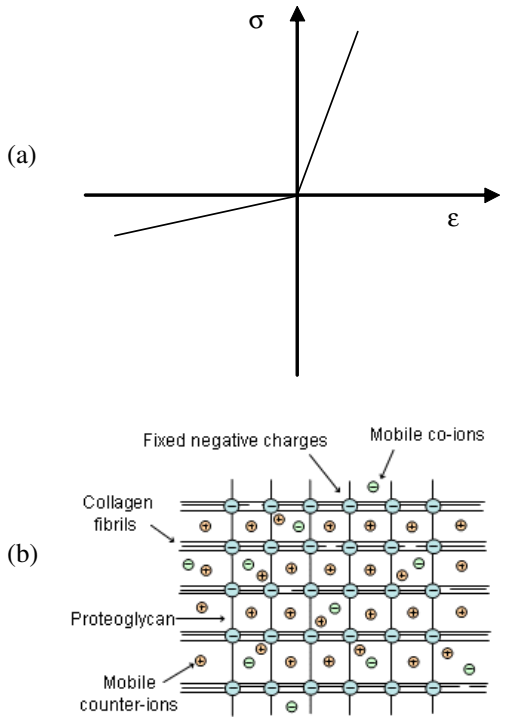

Figure 2 : (a) Cartilage tension-compression nonlinearity, (b) A schematic representation of structure-function relation of the collagen-proteoglycan network, interplaying with fixed negative charges in the PG molecules and mobile ions.

For many years, the ECM is known to be heterogeneous with a sparse distribution of chondrocytes distributed throughout a dense collagen-proteoglycan solid matrix. A schematic of the proteoglycan molecular structure, and the location of the charges on the molecule, and its relationship relative to the cells are shown in Fig. 1a and 1b. The charges on this macromolecule provide the motive force (osmotic pressure) necessary for tissue hydration, and its avidity for water endows the ECM with extremely low permeabilities e.g. [Gu, Yao, Huang et al. (2003); Mow, Gu and Chen (2005)]. Because the ECM is a mixture of collagen fibrous network and proteoglycan gel, cartilage is known to have different properties in tension and in compression, possibly with two orders of magnitude difference, Fig. 2a. This characteristic of the tissue is known as the tension-compression nonlinearity (TCN), and is known to manifest itself to profoundly dominate cartilage's response to loading [Soltz and Ateshian (2000); Huang, Soltz, Kopacz et al. (2003)]. Previously, Soltz and Ateshian [Soltz and Ateshian (2000)] incorporated the continuum-based conewise linear elasticity (CLE) model of Curnier and Zysset [Curnier, He and Zysset (1995)] into the constitutive framework of the biphasic theory to describe the cartilage solid matrix, and employed the CLE biphasic model to successfully curve-fit the unique pattern of stress relaxation behavior exhibited by cartilage under the two testing configurations defined by confined compression and unconfined compression. The dramatic difference in the behavior and properties of the tissue that exhibit the tension-compression nonlinearity as compared to those of a linear isotropic material would undoubtedly result in distinctively different MEC fields within the tissue. However, how the chondrocytes respond within such unique MEC fields or mechanically interact with the ECM that exhibit a TCN property has not been characterized to date. In this study, we aim to first develop a triphasic, multi-scale, finite element model incorporating the CLE that can describe the various known coupled mechanical, electrical and chemical events given rise from mobile ions and fixed negative charges, while at the same time representing the tension-compression nonlinearity of the extracellular matrix. (Fig. 2b). The CLE triphasic finite element model will then be used to investigate the MEC interactions between the chondrocytes and the ECM under an unconfined compression, and to characterize the effect of the tissue TCN on the cell's MEC responses. Utilizing the framework of the triphasic constitutive theory, the ef-

fect of the fixed charge density of the cell and the PCM on the cell responses will be further explored parametrically.

2 Materials and Methods

2.1 Material Model

Cartilage extracellular matrix, pericellular matrix and the chondrocytes were modeled as triphasic mixtures, consisting of a charged permeable and deformable solid phase, an interstitial fluid phase, and ion phases including cat-ions and anions. The formulations used in the model are based on the triphasic theory [Lai, Hou and Mow (1991)] that has been shown to successfully describe the viscoelastic behavior of biological tissue; in this theory the mechanism of energy dissipation results from the resistance of the extracellular matrix to interstitial fluid flow. The physicochemical effect from the charges fixed onto the proteoglycan molecules (Fig. 1a) is an osmotic pressure (known as Donnan osmotic pressure; see [Mow, Gu and Chen (2005)]) effect due to the excess of total mobile ion concentration within the tissue above the mobile ion concentration in the external solution. In a triphasic material, the constitutive relation for the total mixture stress can be written as $\sigma = -p\mathbf{I} + \sigma^e$, which is the sum of the interstitial fluid pressure p that includes osmotic pressure, and the elastic stress σ^e resulting from deformation of the solid matrix. In this study, the chondrocyte and its surrounding PCM are considered to have a homogeneous, linearly isotropic elastic solid phase, in which case the elastic stress $\sigma^e = \lambda_s e\mathbf{I} + 2\mu_s\mathbf{E}$ where λ_s and μ_s are the intrinsic Lame's constants for the elastic solid matrix. The strain tensor $\mathbf{E}$ represents the infinitesimal strains of the solid phase, and e is its trace, also known as the dilatation of solid matrix.

While Curnier and Zysset's CLE model for an elastic solid was adopted by Soltz and Ateshian to be used in the biphasic theory [Soltz and Ateshian (2000)], in this study, the CLE model is now incorporated into the triphasic theory so as to be able to analyze both the influence of TCN and charged characteristics on cartilage ECM behavior. The bimodular response of cartilage described by the CLE model is a manifestation of the fibrillar nature of the collagen matrix. Since the tensile modulus of cartilage differ along directions parallel and perpendicular to the split lines [Huang, Soltz, Kopacz et al. (2003); Huang, Stankiewicz, Ateshian et al. (2005)], the orthotropic symmetry according to the "orthotropic octantwise linear elasticity" from Curnier and Zysset's theory was chosen to represent the plane of symmetry resulting from the orthotropic collagen fibrillar bundles orientations. The three preferred directions are chosen to be 1) parallel to the split line direction, 2) perpendicular to the split line direction and 3) perpendicular to the cartilage surface, (See [Mow, Gu and Chen (2005)] for a discussion of split lines on the articular cartilage surface). The mixture stress is then a function of a texture tensor in such a way that the compressive or tensile material parameter λ_s in each preferred direction are selected according to the state (compressive or tensile) of strain component for the corresponding direction;

$$\sigma^e_{11} = (\lambda_{11}\{E_{11}\} + 2\mu_1)E_{11} + \lambda_{12}E_{22} + \lambda_{13}E_{33}, \tag{1}$$

$$\sigma^e_{22} = \lambda_{12}E_{11} + (\lambda_{22}\{E_{22}\} + 2\mu_2)E_{22} + \lambda_{23}E_{33}, \tag{2}$$

$$\sigma^e_{33} = \lambda_{13}E_{11} + \lambda_{23}E_{22} + (\lambda_{33}\{E_{33}\} + 2\mu_3)E_{33}, \tag{3}$$

where $\lambda_{aa}\{E_{aa}\} = \lambda_{-aa}$ if $E_{aa} < 0$ or $\lambda_{aa}\{E_{aa}\} = \lambda_{+aa}$ if $E_{aa} > 0$, $a = 1,2,3$.

To simplify the problem, the material symmetry was approximated as cubic symmetry to reduce the number of required material constants from twelve to four, designated as followed;$\lambda_{-11} = \lambda_{-22} = \lambda_{-33} = \lambda_{-1}, \lambda_{+11} = \lambda_{+22} = \lambda_{+33} = \lambda_{+1}, \lambda_{23} = \lambda_{13} = \lambda_{12} = \lambda_2and\mu_1 = \mu_2 = \mu_3 = \mu$.

2.2 Multi-scale Finite Element Model

An axisymmetric finite element model based on the triphasic theory [Sun, Gu, Guo et al. (1999)] was used to analyze an inclusion of the chondrocyte surrounded by the pericellular matrix and embedded within the cartilage extracellular matrix under an unconfined compression configuration (Fig. 3). A multi-scale numerical algorithm following the procedure used by Guilak and Mow [Guilak and Mow (2000)] was employed for the computational analyses at both the tissue and cell levels (Fig. 3). In this algorithm, a finite element analysis of the macro-scale problem was first performed to determine the main variables (solid displacements, fluid velocities, and modified terms of chemical potentials according to [Sun, Gu, Guo et al. (1999)] at each node in a model representing the entire cartilage explants. The results of

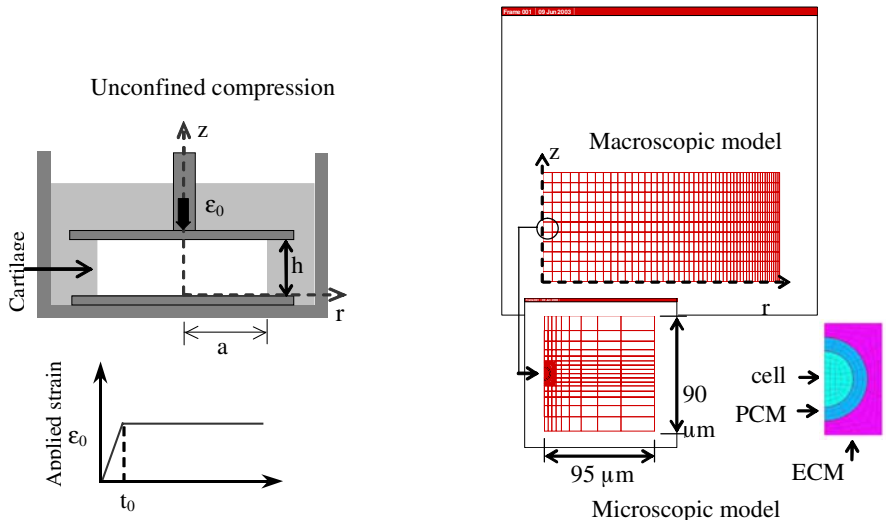

Figure 3 : Multi-scale finite element model of articular cartilage under unconfined compression. (left) A cylindrical cartilage explant between two rigid frictioniless, non-permeable platens submerged in a saline solution of 0.15M (a = 2.4 mm, h = 1 mm), applied with a ramped (t_0= 200s) compressive strain (ε_0=10%). (right) Model of chondrocyte surrounded by the PCM (2.5 μm thick) and embedded within the local cartilage ECM.

this macro-scale finite element analysis were then used to define the applied boundary conditions of a separate micro-scale finite element model (Fig. 3).

The macro-scale problem was chosen to be that of an axisymmetric cylindrical disc of articular cartilage (4.8 in diameter, 1 mm thick) compressed under a ramp displacement load (10% surface-to-surface strain, ramp speed 0.05%/s) between two rigid, frictionless, impermeable platens. The macro-scale mesh consisted of 550 bilinear elements and 612 nodes. The micro-scale model (96$\times$91 μm section) represented an inclusion of the chondrocyte (10 μm diameter) surrounded by the PCM (2.5 μm thick) within the local ECM that located at the middle layer along the central axis of the macro-scale model. The micro-scale mesh consisted of 252 bilinear elements and 287 nodes. The boundary conditions at the lateral edge of the tissue were; radial stress equals to zero and the ion concentrations equals to the outside saline solution of 0.15M. At the central axis the radial solid displacement, fluid flux and ion fluxes were zero.

The multi-scale FEM was used to simulate the chondrocyte deformational response and the MEC environment of the cell. A set of realistic and physiologically normal values available in the current literatures for the intrinsic parameters of the ECM, PCM and chondrocyte were selected, as shown in Table 1. The ECM intrinsic properties were approximated from Soltz and Ateshian, 2000 [Soltz and Ateshian (2000)] where bovine cartilage moduli and permeability were curve-fitted from experimental data obtained from multiple testing configurations, using the biphasic CLE model. The aggregate modulus and permeability of the PCM were obtained from the micropipette aspiration tests on human chondron performed by Alexopoulos and coworkers [Alexopoulos, Haider, Vail et al. (2003); Alexopoulos, Williams, Upton et al. (2005)], and those of chondrocytes were approximated from an unconfined creep compression test on bovine chondrocytes reported by Leipzig and coworkers [Leipzig and Athanasiou (2005)].

The effect of the tension-compression nonlinearity of the cartilage ECM on the chondrocyte responses was investigated by comparing results from the model with the ECM considered as a CLE triphasic material, to those from the model with the ECM considered as a linear isotropic triphasic material. For the latter case, the aggregate modulus of 0.4 MPa and Poisson's ratio of 0.2 were used for the ECM for all direction, chosen from baseline values of cartilage properties widely available in the literature, e.g. see review by [Mow, Gu and Chen (2005)], where the tissue was mostly modeled as a linear isotropic biphasic material. Further more, the effect of the cell and PCM fixed charge density on the cell deformation characteristic was investigated parametrically by varying the values of the cell and PCM fixed charge

Table 1 : Material parameters employed in the model

	ν_+	ν_-	H_{a+} (MPa)	H_{a-} (MPa)	μ (MPa)	λ_{+1} (MPa)	λ_{-1} (MPa)	λ_2 (MPa)	k (m^4/Ns)	ϕ_w	FCD (mEq/ml)
ECM	0.43	0.03	13.1	0.64	0.17	12.8	0.3	0.48	6×10^{-16}	0.75	0.2

	ν	H_a (kPa)	μ (kPa)	λ (kPa)	k (m^4/Ns)	ϕ_w	FCD (mEq/ml)
PCM	0.04	40.0	19.2	1.7	5×10^{-17}	0.7	0.0 - 0.25
Cell	0.07	3.0	1.4	0.2	5×10^{-12}	0.6	0.05 – 0.2

density within a physiological range of 0.05-0.2 mEq/ml for the cell and 0.0-0.25 mEq/ml for the PCM, as shown in Table 1 [Maroudas (1979); Poole, Glant and Schofield (1991)]. Finally, the effect of presence of the PCM was also characterized by comparing the MEC field results from models with and without the PCM.

3 Results

As is well known, cartilage tissue exhibits time-dependent behaviors under compression due to fluid exudation from the lateral edge of the tissue [Armstrong, Lai and Mow (1984)]. Under applied 10% axial strain by rigid frictionless platens in unconfined compression, the tissue expanded laterally independent of the depth, then recoiled gradually until reached an equilibrium state. The equilibrium lateral expansion of cartilage depends on the intrinsic Poisson's ratio and the Donnan osmotic pressure effect due to presence of fixed negative charges in the tissue [Sun, Guo, Likhitpanichkul et al. (2004); Wan, Miller, Guo et al. (2004)].

The time-dependent deformation and volume change responses of the chondrocyte located at the center of the tissue disc are shown in Fig. 4 in terms of the axial diameter (Fig. 4a), the radial diameter (Fig. 4b) and the volume (Fig. 4c), with all values normalized by the original dimension. These graphs show a comparison of the cell response to the response of the ECM at the boundary of the micro-scale, to demonstrate how the deformation transmitted from the local ECM to the cell occurred. The results from the CLE-triphasic model were also compared to those from the linear-isotropic triphasic model to characterize the effect of the ECM tension-compression nonlinearity on the cell responses, as shown in Fig. 4a. At equilibrium the cell deformed about 20% axially under the applied axial strain of 10% on the tissue, for both the CLE model and the linear model. Radially (Fig. 4b), the ECM expanded during the ramp period then dramatically recoiled to almost the original dimension for the CLE model, while only recoiled slightly for the linear model. The tissue radial deformation induced the cell radial diameter to change in a similar characteristic for both models. In the linear case, the cell radial expansion was about 5% more than that of the ECM, while in the CLE case, the cell expansion peak was significantly higher than that of the ECM, and the cell recoiled beyond the original dimension at equilibrium. Interestingly, the chondrocyte volume in the CLE model increased during the ramp period, then decreased to 80% of its original volume at equilibrium, while it monotonically decreased to 94% of its original volume in the linear case.

The triphasic multi-scale FEM model allowed determination of not only mechanical environment of the cell, but also the osmolarity around the cell and the electric potential across the cell membrane (Fig. 5a-d). As expected, differences in the mechanical behaviors and properties of the cell and the ECM led to dramatic differences in the cell mechano-electrochemical environment. The dilatation of the chondrocyte was positive during the ramp loading period, then became negative with an increased magnitude up to 0.2 at equilibrium. The dilatation contour plot showed that a negative dilatation in the tissue propagated to the cell radially during the transient response, and resulted in an amplified dilatation inside the cell at equilibrium (Fig. 5a). The fluid pressure distribution was found to be quite uniform across the tissue to the cell, with a high pressurization occurred initially and diminished to zero at equilibrium (Fig. 5b). The unconfined compression loading induced an increase in osmolarity in the local tissue region, with the value of 380 mOsm at equilibrium, as compared to the initial value of 300 mOsm. There was a gradient of osmolarity from the ECM to the PCM to the cell, with the highest value of 400 mOsm inside the PCM region, and the lowest value of 330 mOsm inside the cell, at equilibrium (Fig. 5c). A gradient of electric potential across the ECM, PCM

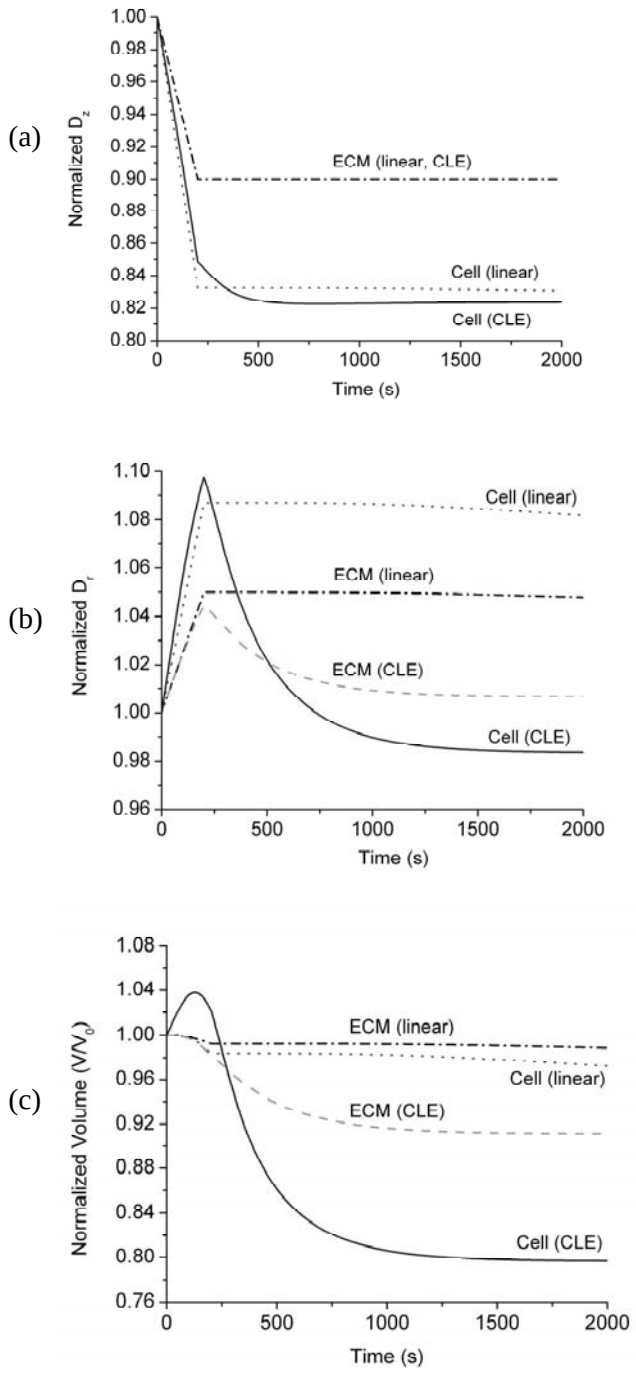

Figure 4 : Comparison of cell and ECM deformation results from the CLE model to those from linear model, where FCD_{cell} = 0.1, mEq/ml, FCD_{PCM} = 0.25 mEq/ml. (a) Normalized axial dimension, (b) Normalized radial dimension and (c) Normalized volume.

and the cell was also observed, with the highest value always inside the cell and the lowest value always in the PCM; thus it is likely that local electrical currents will exist around the cell. The electric potential difference across the cell and the PCM increased from about -13 mV at the peak ramp to -8 mV at equilibrium.

Figure 6 showed the effect of the cell fixed charge density on the cell deformational responses. It can be clearly seen that different values of cell FCD generated different characteristics in the transient response of the cell axial deformation (Fig. 6a), modulated the equilibrium value of the radial expansion (Fig. 6b), and overall resulted in significant difference in the cell volume change (Fig. 6c). Higher cell FCD increased the equilibrium values of the deformations and volume, while lower FCD dramatically decreased them. The equilibrium volume change reduced from 80% to 70% of the original value when the FCD was decreased from 0.1 to 0.05 mEq/ml (Fig. 6c). Interestingly, for cases that the FCD was 0.15 and 0.2 mEq/ml, the axial diameter of the cell recovered to a value in the relaxation period after a reduction to a peak value in the ramp period, while in cases that the FCD was 0.1 and 0.05 mEq/ml, the axial diameter decreased during the ramp period then further decreased monotonically until reaching equilibrium (Fig. 6a).

Without the PCM, we found that the effect of the cell FCD on the cell radial expansion diminished (Fig. 7b). However, the effect of the cell FCD on the transient characteristic of the cell axial deformation still remained, with a slight reduction of the effect on the equilibrium value (Fig. 7a). This result induced a smaller effect of the cell FCD on the equilibrium value of the overall cell volume change (Fig. 7c). The FCD of the PCM was also found to have significant effect on the cell deformational response. With smaller value of FCD in the PCM, the cell radial diameter recoiled much less than that of higher FCD value (Fig. 8b). For instance, the equilibrium value of the normalized radial diameter increased from 0.98 to 1.08, when the FCD of the PCM was reduced from 0.25 to 0.0 mEq/ml. Further more, the FCD value of the PCM characterized the transient response in the cell axial deformation to either monotonically reduced to an equilibrium value (FCD higher than 0.2 mEq/ml) or initially reduced and then recovered to a value (FCD less than 0.1 mEq/ml) (Fig. 8a).

4 Discussion

The tension-compression nonlinearity is an important property of articular cartilage and has been shown to play

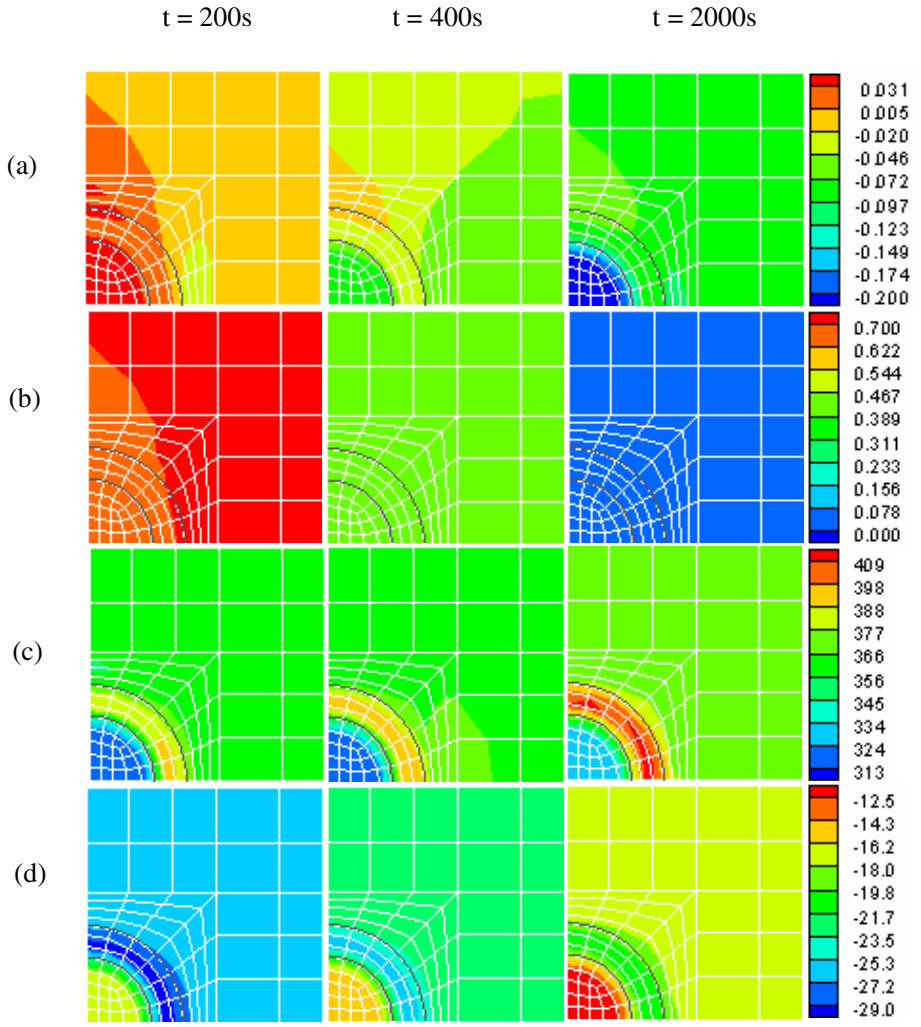

Figure 5 : Contour plots from the micro-scale model results of (a) the dilatation, (b) the fluid pressure, Pa, (c) the osmolarity, mOsm and (d) the electric potential, mV. FCD_{cell} = 0.1 mEq/ml, FCD_{PCM} = 0.25 mEq/ml.

a major role in its load-bearing function. In this study, we created a multi-scale CLE-triphasic finite element model that accounts for the TCN of the extracellular matrix to investigate how this property of the tissue affects the deformational responses of the chondrocytes, which will lead to more insights in understanding the mechanisms of mechano-transduction. The CLE-triphasic model also allowed analysis of the osmotic and electro-kinetic events given rise by interplay of mobile ions in the physiological interstitial fluid and fixed negative charges in the proteoglycan molecule inside the ECM and PCM, as well as the cytoskeleton of the cell.

Results from model simulations showed that the cell deformational responses, in both radial and axial direction, were highly time dependent during both the ramp period and the relaxation period. It was also clearly shown that the characteristic of the cell deformation and volume change when the cell was embedded within the ECM that exhibited tension-compression nonlinearity was remarkably different from when it was within a linear isotropic material (Fig. 4). Calculations of the cell axial diameter from the triphasic-CLE model further reduced significantly even when the axial deformation of the cartilage ECM itself was kept constant, while only slightly decreased further in the linear model (Fig. 4a). Within a TCN material with low compressive Poisson's ratio, the ECM expanded and recoiled to almost its original dimension and induced the cell to expand and recoil laterally in

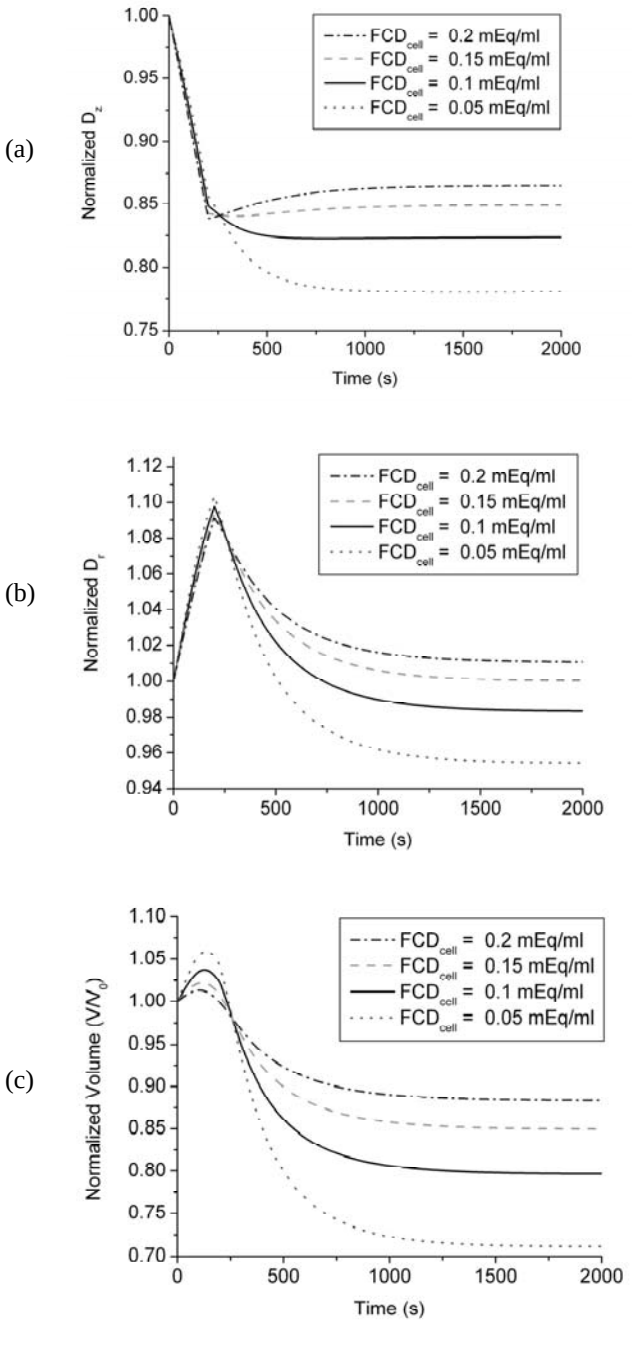

Figure 6 : Effect of the cell fixed charge density on the cell deformational response, with presence of the PCM, where FCD_{PCM} = 0.2 mEq/ml. . (a) Normalized axial dimension, (b) Normalized radial dimension and (c) Normalized volume.

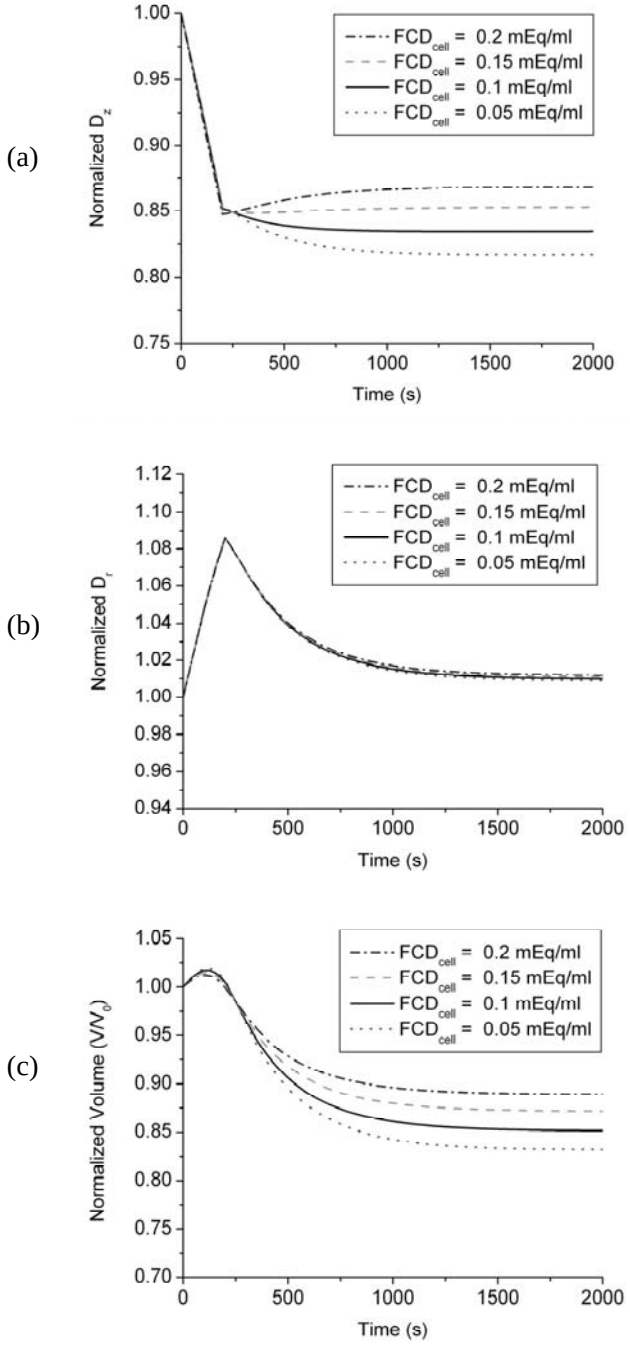

Figure 7 : Effect of the cell fixed charge density on the cell deformational response, without presence of the PCM. (a) Normalized axial dimension, (b) Normalized radial dimension and (c) Normalized volume.

a similar manner (Fig. 4b). The cell responses during the ramp period resulted from transduction of axial compressive stress and radial tensile stress generated within the ECM. During this initial period, high fluid pressure occurred within the ECM at the central axis of the cartilage disc, as well as inside the cell and the PCM in this

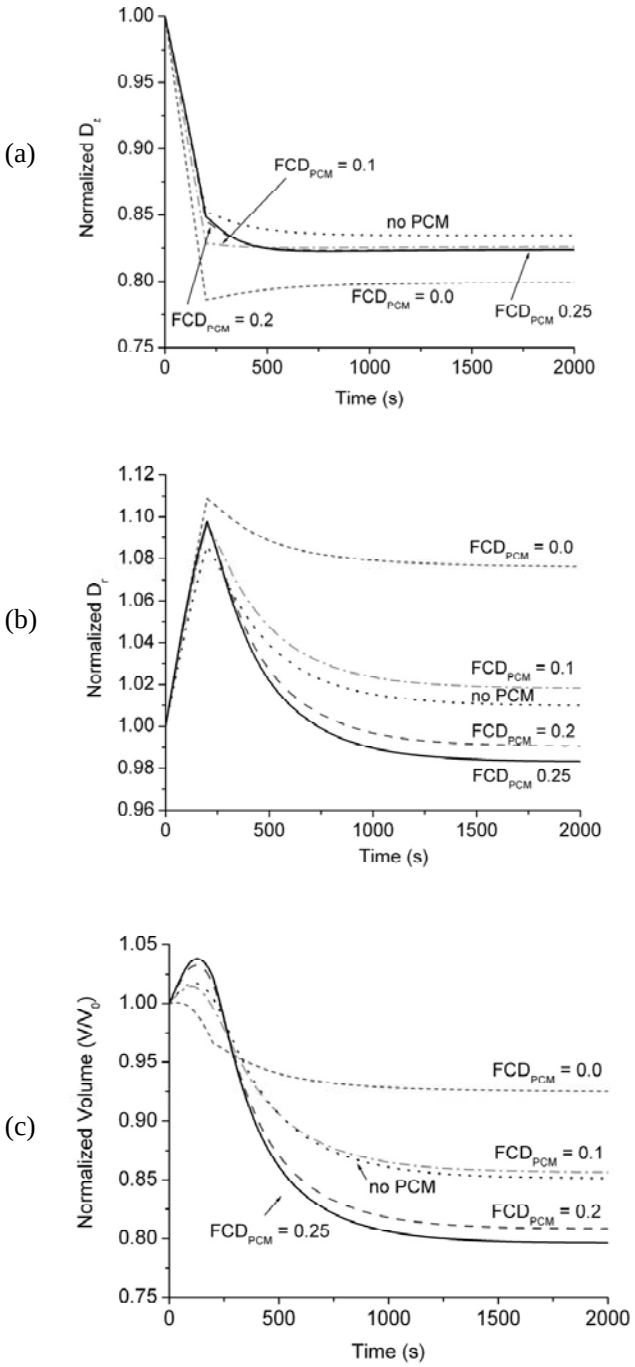

Figure 8 : Effect of fixed charge density of the PCM on the cell deformation, where FCD_{cell} = 0.1 mEq/ml. (a) Normalized axial dimension, (b) Normalized radial dimension and (c) Normalized volume.

region (Fig. 5b). When the lateral fluid exudation of the tissue propagated to the central area, the fluid pressure in the local ECM reduced, and the fluid inside the cell escaped. The cell fluid exudation resulted in further decrease in the cell axial diameter, and the transient reduction of the axial diameter was controlled by the permeability of the cell, the PCM and the ECM. The overall cell volume turned out to increase slightly during the ramp period since the lateral expansion dominated the axial compression. During the relaxation period, further reduction of the cell axial diameter combined with the dramatic recoil of the radial diameter resulted in a significant decrease of the cell volume. At equilibrium, the cell volume decreased by 20 % in the CLE model which was several times larger than the volume change in the linear case. The quantitative information of the cell deformation and volume change provided in this study is valuable for analysis of the mechanical response interrelating with the role of membrane receptors, such as integrins, and the stretch-activated ion channels, which are considered as putative mechanical signal transducers for chondrocytes [Mobasheri, Carter, Martin-Vasallo et al. (2002)].

In addition, it was found that changes in both the axial and radial diameters of the cell were further modulated by the FCD of the cell. As shown in Fig. 6a, the cell axial diameter decreased during the ramp period in all values of FCD, then recovered to a value in cases that the cell FCD was 0.15 and 0.2 mEq/ml, and further decreased when the cell FCD was 0.1 and 0.05 mEq/ml. This phenomenon can be explained as followed; higher value of FCD induced higher Donnan osmotic pressure and influenced the cell to behave like a stiffer material with higher Poisson's ratio, hence the cell axial diameter expanded while the radial diameter was being compressed by the ECM during the recoiling process of the tissue. The effect of the FCD on a triphasic material's apparent modulus and apparent Poisson's ratio under unconfined compression has been thoroughly described by Wan and coworkers [Wan, Miller, Guo et al. (2004)]. The dependency of distinct characteristic curves of the cell transient axial deformation on the cell FCD can provide a clue to approximate the value of the cell FCD by measuring the cell diameter in cartilage under unconfined compression.

For the radial deformation, the cell expanded during the ramp period and recoiled during the relaxation period in all cases of cell FCD. However, the radial diameter of cells with FCD of 0.1 mEq/ml and 0.05 mEq/ml recoiled beyond the original dimension. The effect of the FCD on

the radial deformation can be explained in a similar manner; lower FCD induced lower Donnan osmotic pressure and modulated the material to behave like a softer material, hence the deformation of the cell resulting from lateral compression exerted by the ECM during the recoiling process of the tissue was larger. The dramatic recoil beyond its original dimension was later found to be mainly due to the effect of the PCM, as it was clearly shown that without the PCM the cell radial diameter did not recoil beyond the original dimension in all cases of the cell FCD (Fig. 7b). This effect clearly showed the role of the PCM and was most likely due to the gradual change of the material modulus from the ECM to the PCM to the cell, as opposed to an extreme drop from the ECM directly to the cell. On the other hand, from Fig. 7a, the axial diameter of the cell was still affected by the cell FCD in a similar manner as in the case when the PCM was presented, which further confirmed that this phenomenon was mainly modulated by properties of the cell itself.

The FCD of the PCM was also found to play an important role in the cell deformational response. The cell radial deformation recoiled beyond its original dimension only in cases that the FCD of the PCM were 0.2 or 0.25 mEq/ml, and the recoil decreased as the FCD of the PCM was reduced (Fig. 8b). The characteristic of the cell axial deformation were also dictated by the FCD value of the PCM. For PCM with FCD higher than 0.1 mEq/ml, the cell axial diameter further decreased during the relaxation time, while PCM with lower FCD modulated the axial diameter to recover (Fig. 8a). Overall, the cell volume change was increased from the case without the PCM when the FCD of the PCM was higher than 0.1 mEq/ml (Fig. 8c). Physiological PG content suggested that the FCD of the PCM is higher than that of the ECM [Maroudas (1979); Poole, Glant and Schofield (1991)], hence it is most likely that the PCM will play a role in amplifying the cell volume change.

In conclusion, a CLE triphasic multi-scale finite element was developed for this study. The effect of the tension-compression nonlinearity of cartilage tissue on the cell responses within the unconfined compression configuration were characterized, and the computational results confirmed that this important property of the tissue must not be neglected in order to accurately determine the MEC interaction between the cell and the matrix. The results from the model clearly showed that experiments over the past decades on defining tissue composition, collagen and proteoglycan organization and ultrastructure, ECM mechanical properties, and cellular distribution and location within the tissue all have significant effects on the cell-ECM mechano-electrochemical interactions. Moreover, the MEC fields around and in the cells are all time dependent. Hence any interpretations based on static and linear isotropic models on cell-ECM interactions are bound to be misleading at best or at worst wrong. However, with modeling procedures described here, one can now move forward with well crafted experiments coupled with better computational models to untangle the various basic issues that are involved in the mechanically, electrically and chemically induced signal transduction processes for the regulation of tissue growth and degeneration.

Acknowledgement: This study was supported by NIH Grants No. AR41913 and AR42850, and the Whitaker Foundation Special Development Award.

References

Alexopoulos, L. G.; Haider, M. A.; Vail, T. P.; Guilak, F. (2003): Alterations in the mechanical properties of the human chondrocyte pericellular matrix with osteoarthritis. *J Biomech Eng*, vol. 125, pp. 323-33.

Alexopoulos, L. G.; Williams, G. M.; Upton, M. L.; Setton, L. A.; Guilak, F. (2005): Osteoarthritic changes in the biphasic mechanical properties of the chondrocyte pericellular matrix in articular cartilage. *J Biomech*, vol. 38, pp. 509-17.

Armstrong, C. G.; Lai, W. M.; Mow, V. C. (1984): An analysis of the unconfined compression of articular cartilage. *J Biomech Eng*, vol. 106, pp. 165-73.

Bachrach, N. M.; Valhmu, W. B.; Stazzone, E.; Ratcliffe, A.; Lai, W. M.; Mow, V. C. (1995): Changes in proteoglycan synthesis of chondrocytes in articular cartilage are associated with the time-dependent changes in their mechanical environment. *J Biomech*, vol. 28, pp. 1561-9.

Buschmann, M. D.; Gluzband, Y. A.; Grodzinsky, A. J.; Hunziker, E. B. (1995): Mechanical compression modulates matrix biosynthesis in chondrocyte/agarose culture. *J Cell Sci*, vol. 108 (Pt 4), pp. 1497-508.

Chao, P. H.; Roy, R.; Mauck, R. L.; Liu, W.; Valhmu, W. B.; Hung, C. T. (2000): Chondrocyte translocation

response to direct current electric fields. *J Biomech Eng*, vol. 122, pp. 261-7.

Curnier, A.; He, Q.-C.; Zysset, P. (1995): Conewise linear elastic materials. *J Elast*, vol. 37, pp. 1-38.

Goodier, J. (1937): Concentration of stress around spherical and cylindrical inclusions and flaws. *J Appl Mech*, vol. 55, pp. 39-44.

Gu, W. Y.; Yao, H. (2003): Effects of hydration and fixed charge density on fluid transport in charged hydrated soft tissues. *Ann Biomed Eng*, vol. 31, pp. 1162-70.

Gu, W. Y.; Yao, H.; Huang, C. Y.; Cheung, H. S. (2003): New insight into deformation-dependent hydraulic permeability of gels and cartilage, and dynamic behavior of agarose gels in confined compression. *J Biomech*, vol. 36, pp. 593-8.

Guilak, F.; Sah, R. L.; Setton, L. A., (1997), Physical regulation of cartilage metabolism, In: V. C. Mow, and W. C. Hayes (ed). *Basic orthopaedic biomechanics*, Philadelphia, pp. 179-207.

Guilak, F.; Mow, V. C. (2000): The mechanical environment of the chondrocyte: a biphasic finite element model of cell-matrix interactions in articular cartilage. *J Biomech*, vol. 33, pp. 1663-73.

Heinegard, D.; Bayliss, M.; Lorenzo, P., (2003), Pathogenesis of structural changes in the osteoarthritic joint, In: K. D. Brandt, M. Doherty, and L. S. Lohmander (ed). *Osteoarthritis*, pp. 73-82.

Huang, C. Y.; Soltz, M. A.; Kopacz, M.; Mow, V. C.; Ateshian, G. A. (2003): Experimental verification of the roles of intrinsic matrix viscoelasticity and tension-compression nonlinearity in the biphasic response of cartilage. *J Biomech Eng*, vol. 125, pp. 84-93.

Huang, C. Y.; Stankiewicz, A.; Ateshian, G. A.; Mow, V. C. (2005): Anisotropy, inhomogeneity, and tension-compression nonlinearity of human glenohumeral cartilage in finite deformation. *J Biomech*, vol. 38, pp. 799-809.

Hung, C. T.; LeRoux, M. A.; Palmer, G. D.; Chao, P. H.; Lo, S.; Valhmu, W. B. (2003): Disparate aggrecan gene expression in chondrocytes subjected to hypotonic and hypertonic loading in 2D and 3D culture. *Biorheology*, vol. 40, pp. 61-72.

Jin, M.; Frank, E. H.; Quinn, T. M.; Hunziker, E. B.; Grodzinsky, A. J. (2001): Tissue shear deformation stimulates proteoglycan and protein biosynthesis in bovine cartilage explants. *Arch Biochem Biophys*, vol. 395, pp. 41-8.

Lai, W. M.; Hou, J. S.; Mow, V. C. (1991): A triphasic theory for the swelling and deformation behaviors of articular cartilage. *J Biomech Eng*, vol. 113, pp. 245-58.

Lai, W. M.; Sun, D. D.; Ateshian, G. A.; Guo, X. E.; Mow, V. C. (2002): Electrical signals for chondrocytes in cartilage. *Biorheology*, vol. 39, pp. 39-45.

Lammi, M. J.; Inkinen, R.; Parkkinen, J. J.; Hakkinen, T.; Jortikka, M.; Nelimarkka, L. O.; Jarvelainen, H. T.; Tammi, M. I. (1994): Expression of reduced amounts of structurally altered aggrecan in articular cartilage chondrocytes exposed to high hydrostatic pressure. *Biochem J*, vol. 304 (Pt 3), pp. 723-30.

Leipzig, N. D.; Athanasiou, K. A. (2005): Unconfined creep compression of chondrocytes. *J Biomech*, vol. 38, pp. 77-85.

Maroudas, A., (1979), Physicochemical properties of articular cartilage., In: M. A. R. Freeman ed., *Adult Articular Cartilage*, Kent, UK, pp. 215-290.

Mauck, R. L.; Soltz, M. A.; Wang, C. C.; Wong, D. D.; Chao, P. H.; Valhmu, W. B.; Hung, C. T.; Ateshian, G. A. (2000): Functional tissue engineering of articular cartilage through dynamic loading of chondrocyte-seeded agarose gels. *J Biomech Eng*, vol. 122, pp. 252-60.

Mobasheri, A.; Carter, S. D.; Martin-Vasallo, P.; Shakibaei, M. (2002): Integrins and stretch activated ion channels; putative components of functional cell surface mechanoreceptors in articular chondrocytes. *Cell Biol Int*, vol. 26, pp. 1-18.

Mow, V. C.; Kuei, S. C.; Lai, W. M.; Armstrong, C. G. (1980): Biphasic creep and stress relaxation of articular cartilage in compression: Theory and experiments. *J Biomech Eng*, vol. 102, pp. 73-84.

Mow, V. C.; Wang, C. C.; Hung, C. T. (1999): The extracellular matrix, interstitial fluid and ions as a mechanical signal transducer in articular cartilage. *Osteoarthritis Cartilage*, vol. 7, pp. 41-58.

Mow, V. C.; Gu, W. Y.; Chen, F. H., (2005), Structure and function of articular cartilage and meniscus, In: V. C. Mow, and R. Huiskes (ed). *Basic orthopaedic biomechanics and mechano-biology*, Philadelphia, pp. 181-258.

Palmer, G. D.; Chao Ph, P. H.; Raia, F.; Mauck, R. L.;

Valhmu, W. B.; Hung, C. T. (2001): Time-dependent aggrecan gene expression of articular chondrocytes in response to hyperosmotic loading. *Osteoarthritis Cartilage*, vol. 9, pp. 761-70.

Poole, C. A.; Glant, T. T.; Schofield, J. R. (1991): Chondrons from articular cartilage. (IV). Immunolocalization of proteoglycan epitopes in isolated canine tibial chondrons. *J Histochem Cytochem*, vol. 39, pp. 1175-87.

Quinn, T. M.; Grodzinsky, A. J.; Buschmann, M. D.; Kim, Y. J.; Hunziker, E. B. (1998): Mechanical compression alters proteoglycan deposition and matrix deformation around individual cells in cartilage explants. *J Cell Sci*, vol. 111 (Pt 5), pp. 573-83.

Ratcliffe, A.; Beauvais, P. J.; Saed-Nejad, F. (1994): Differential levels of synovial fluid aggrecan aggregate components in experimental osteoarthritis and joint disuse. *J Orthop Res*, vol. 12, pp. 464-73.

Sandy, J. D.; Adams, M. E.; Billingham, M. E.; Plaas, A.; Muir, H. (1984): In vivo and in vitro stimulation of chondrocyte biosynthetic activity in early experimental osteoarthritis. *Arthritis Rheum*, vol. 27, pp. 388-97.

Soltz, M. A.; Ateshian, G. A. (2000): A Conewise Linear Elasticity mixture model for the analysis of tension-compression nonlinearity in articular cartilage. *J Biomech Eng*, vol. 122, pp. 576-86.

Sun, D. D.; Guo, X. E.; Likhitpanichkul, M.; Lai, W. M.; Mow, V. C. (2004): The influence of the fixed negative charges on mechanical and electrical behaviors of articular cartilage under unconfined compression. *J Biomech Eng*, vol. 126, pp. 6-16.

Sun, D. N.; Gu, W. Y.; Guo, X. E.; Lai, W. M.; Mow, V. C. (1999): A mixed finite element formulation of triphasic mechano-electrochemical theory for charged, hydrated biological soft tissues. *Int J Num Meth Engng*, vol. 45, pp. 1375-1402.

Szafranski, J. D.; Grodzinsky, A. J.; Burger, E.; Gaschen, V.; Hung, H. H.; Hunziker, E. B. (2004): Chondrocyte mechanotransduction: effects of compression on deformation of intracellular organelles and relevance to cellular biosynthesis. *Osteoarthritis Cartilage*, vol. 12, pp. 937-46.

Waldman, S. D.; Spiteri, C. G.; Grynpas, M. D.; Pilliar, R. M.; Kandel, R. A. (2003): Long-term intermittent shear deformation improves the quality of cartilaginous tissue formed in vitro. *J Orthop Res*, vol. 21, pp. 590-6.

Wan, L. Q.; Miller, C.; Guo, X. E.; Mow, V. C. (2004): Fixed electrical charges and mobile ions affect the measurable mechano-electrochemical properties of charged-hydrated biological tissues: The articular cartilage paradigm. *Mechanics & Chemistry of Biosystems*, vol. 1, pp. 81-99.

Wang, C. C.; Guo, X. E.; Sun, D.; Mow, V. C.; Ateshian, G. A.; Hung, C. T. (2002): The functional environment of chondrocytes within cartilage subjected to compressive loading: a theoretical and experimental approach. *Biorheology*, vol. 39, pp. 11-25.

Wang, C. C.; Chahine, N. O.; Hung, C. T.; Ateshian, G. A. (2003): Optical determination of anisotropic material properties of bovine articular cartilage in compression. *J Biomech*, vol. 36, pp. 339-53.

Wong, M.; Wuethrich, P.; Buschmann, M. D.; Eggli, P.; Hunziker, E. (1997): Chondrocyte biosynthesis correlates with local tissue strain in statically compressed adult articular cartilage. *J Orthop Res*, vol. 15, pp. 189-96.

Wu, J. Z.; Herzog, W. (2000): Finite element simulation of location- and time-dependent mechanical behavior of chondrocytes in unconfined compression tests. *Ann Biomed Eng*, vol. 28, pp. 318-30.

Wu, Q. Q.; Chen, Q. (2000): Mechanoregulation of chondrocyte proliferation, maturation, and hypertrophy: ion-channel dependent transduction of matrix deformation signals. *Exp Cell Res*, vol. 256, pp. 383-91.